Check for updates

Plant, Cell & Environment

WILEY

Plant, Cell & Environment

ORIGINAL ARTICLE

Intraspecific Variation on Thermal Acclimation of *Phragmites australis*, a Widespread Wetland Plant Species in Response to Multiple Time-Scale Temperature Changes

Linjing Ren[1,2] | Emil Jespersen[2] | Maja B. Juulsager[2] | Wen-Yong Guo[3] | Yanlong He[4] | Hans Brix[2] | Xiuzhen Li[1] | Brian K. Sorrell[2] | Franziska Eller[2]

[1]State Key Laboratory of Estuarine and Coastal Research, East China Normal University, Shanghai, China | [2]Department of Biology, Aarhus University, Aarhus, Denmark | [3]Zhejiang Tiantong Forest Ecosystem National Observation and Research Station, Institute of Eco-Chongming and Research Center for Global Change and Ecological Forecasting, School of Ecological and Environmental Sciences, East China Normal University, Shanghai, China | [4]East China Sea Ecology Center, Ministry of Natural Resources of People Republic of China (MNR), Shanghai, China

Correspondence: Wen-Yong Guo (wyguo@des.ecnu.edu.cn) | Yanlong He (ylhe@ecs.mnr.gov.cn)

Received: 17 July 2024 | **Accepted:** 17 February 2025

Funding: The study was funded by National Natural Science Foundation of China No. 42106166 (to L.R.) and No. 42141016 (to L.R. and X.L.), National Key R&D Program of China No. 2023YFE0113100 (to L.R. and X.L.), China Postdoctoral Science Foundation No. 2021M700043 (to L.R.), Science and Technology Innovation Plan of Shanghai Science and Technology Commission, International Scientific Cooperation No. 22230713100 (to L.R., X.L. and H.B.) and Wet Horizons Horizon Europe GAP-101056848 (to H.B., B.K.S. and F.E.).

Keywords: acclimation | latitudinal pattern | local adaptation | phenotypic plasticity | photosynthesis | thermal optimum

ABSTRACT

The temperature sensitivity of photosynthesis remains a significant uncertainty in wetland plants, critically impacting predictions of vegetation dynamics and ecosystem functions under global warming scenarios. This study investigates the photosynthetic responses of *Phragmites australis*, a model wetland plant with a broad geographic distribution, to temperature variations across three distinct temporal scales. We analysed short-term responses using net photosynthesis rate temperature curves, medium-term acclimation across three growth temperature regimes, and long-term adaptation of phylogeographical groups to their genotypic origins' climate. We demonstrated that the overall photosynthetic performance of *P. australis* is principally driven by thermal acclimation to growth temperature, comparing with local adaptation to climate of origin. Genotypes from diverse geographical regions demonstrated varied physiological strategies: those from higher latitudes exhibited remarkable plasticity, adjusting rapidly to optimise photosynthetic performances under changing thermal conditions. These intraspecific differences highlighted the role of evolutionary history in shaping species' potential resilience and adaptive capacity. This study also underscored the complex interplay between temperature, O_2 sensitivity and photosynthetic efficiency, advancing our understanding of how widespread wetland species respond to ongoing global climate dynamics.

1 | Introduction

The global average surface temperature has risen by approximately 1.1°C above pre-industrial levels and is projected to reach 1.5°C between 2030 and 2035 (IPCC 2018; Climate Champions 2023). This warming climate is expected to significantly impact plant growth and distribution (Bakkenes et al. 2002; Thuiller et al. 2005; Dusenge et al. 2019). In addition, extreme weather events such as heatwaves and droughts are becoming more frequent and severe, leading to competition for

© 2025 John Wiley & Sons Ltd.

resources or even extinction for some species (Turner et al. 2020; Rivero et al. 2022). The climate variability hypothesis (CVH) posits that fluctuations in climate, including temperature patterns, influence various ecological and evolutionary processes, shaping the distribution, adaptation and diversity of species over time (Janzen 1967; Stevens 1989). Understanding large-scale thermal adaptation patterns not only reveals historical and eco-evolutionary processes but also informs predictions about species' responses to future climate changes (Addo-Bediako et al. 2000; Chown et al. 2004; Bennett et al. 2021).

Latitudinal gradients in functional traits and thermal tolerances are commonly used to indicate species' temperature adaptation to local environmental temperatures, underscoring the impact of geographic and climatic variability (Sunday et al. 2019; Lancaster and Humphreys 2020). Within species, adaptation capacity also varies significantly among genetically diverse populations, closely linked to the environmental conditions of their genetic origins (Jump and Peñuelas 2005). However, climate-driven ecological forecasting models like climate envelope models (CEMs) typically operate at a species-wide level, assuming intra-specific genetic uniformity and employing shared tolerance thresholds to outline the climatic constraints of species' geographic shifts due to climate change (Bolnick et al. 2003; Banta et al. 2012; Ikeda et al. 2017). This approach often overlooks the potential for local adaptation, leading to significant variations within species (Angert et al. 2011; Fournier-Level et al. 2011; Wessely et al. 2022). Therefore, advancing research on intraspecific thermal adaptation is crucial for refining predictions of species responses to climate change and developing effective mitigation strategies (Jump and Peñuelas 2005; Aguirre-Liguori et al. 2021).

Populations respond to environmental stresses through physiological, genetic and behavioural mechanisms that operate over varying timescales, influenced by the specific traits being observed, the genetic diversity within the population, and the local environmental conditions (Kristensen et al. 2020, Lancaster and Humphreys 2020). The resilience of plants to global warming depends on their ability to optimise acclimation to the current environmental conditions (Jump and Peñuelas 2005; Miner et al. 2005; Arnold et al. 2019; Aguirre-Liguori et al. 2021). This resilience may vary geographically due to temporal adaption to fine-scale environmental heterogeneity and adaptive genetic specification from long-term natural selection (Joshi et al. 2001; SantamarÍa et al. 2003; Reed et al. 2011). Differentiating between short-term acclimation and long-term adaptation to temperature change is crucial for improving predictions of species resilience and vulnerability (Gerken et al. 2015). Previous studies have shown that acclimation to growth temperature is a more influential factor than adaptation to the climate of origin (Kumarathunge et al. 2019). However, this has not been investigated in widely distributed wetland vegetation.

Phenotypic plasticity, depicted by reaction norms, highlights variations in traits due to short-term environmental changes (Nicotra et al. 2010; Arnold et al. 2019). Analysing these norms across temperature variations and comparing plasticity among genotypes helps unravel the genetic basis of plasticity and evolutionary ecology within a species (Jump and Peñuelas 2005; Valladares et al. 2007; Reed et al. 2011; Arnold et al. 2019). Phenotypic plasticity in intraspecific trait variations has been reported to increase towards high latitudes, where greater climate variability is observed (SantamarÍa et al. 2003; Molina-Montenegro and Naya 2012; Ren et al. 2020). However, observed patterns of phenotypic plasticity are primarily in plant morphology and growth traits, such as height, growth rate, flowering onset, seed mass and germination, leaving knowledge about intraspecific plant ecophysiology and mechanisms underlying plant acclimation to rapid temperature changes and stress mitigation limited (Sasaki and Dam 2019; Aguirre-Liguori et al. 2021).

The response of photosynthesis is crucial for assessing plant health and resilience to thermal stress (Kumarathunge et al. 2019; Crous et al. 2022). Temperature impacts plant photosynthesis by modifying enzymatic activities, especially ribulose-1,5-bisphosphate carboxylase/oxygenase (Rubisco), affecting thylakoid membrane fluidity and chlorophyll stability and regulating stomatal conductance, which collectively influence the rate of photosynthesis by optimising or impairing light-dependent reactions and carbon fixation, with deviations from the thermal optimum also increasing photorespiration and dark respiration rates (Niu et al. 2008; Scafaro et al. 2017; Ren et al. 2025; Wang et al. 2020). Photosynthetic capacity can be evaluated using photosynthetic light response curves (A/I curves), photosynthetic CO_2 response curves (A/C_i curves) and the photosynthesis–temperature curve (A/T curves). A/I curves provide information on electron transport saturation and overall photosynthetic performance, related to irradiance environments at genotypic origins (Ogren 1993). A/C_i curves interpret leaf net assimilation (A) to intercellular CO_2 concentration (C_i), linked to biochemical limitations on photosynthesis and carbon utilization efficiency (Farquhar et al. 1980). Additionally, identifying plastic adjustments in thermal optimum (T_{opt}) through photosynthesis–temperature curves (A/T curves) is crucial for predicting how plant species will adapt or be affected by changing temperatures (Berry and Bjorkman 1980).

Photorespiration is a process that increases with temperature and O_2 concentration, competing with photosynthesis by consuming energy and releasing fixed CO_2, thereby reducing the net photosynthetic rate (Hesketh 1967; Wingler et al. 2000). Studies on the thermal optimum of photosynthesis at a low O_2 concentration can more directly determine how temperature affects the photosynthetic mechanisms, enhancing the accuracy of modelling and predicting plant responses to global warming (Sage and Kubien 2007). In C3 leaves, the sensitivity of A to O_2 and CO_2 can be used to identify photosynthetic limitations, a key distinction for understanding photosynthetic constraints and reducing the impact of uncertainties in the fixed parameters of the Farquhar et al. (1980) model (FvCB) (Sage and Sharkey 1987; Busch and Sage 2017).

Plants widely distributed across strong environmental gradients serve as ideal models for studying intraspecific adaptability to climate change (Bestion et al. 2015; Sasaki and Dam 2019). In this study, we use *Phragmites australis* as a model to assess the temperature response of photosynthesis in widespread wetland plants. We tested the effect of temperature change on photosynthetic capacity across three time scales. The temperature

13653040, 2025, 7, Downloaded from https://onlinelibrary.wiley.com/doi/10.1111/pce.15452 by East China Normal University, Wiley Online Library on [03/06/2025]. See the Terms and Conditions (https://onlinelibrary.wiley.com/terms-and-conditions) on Wiley Online Library for rules of use; OA articles are governed by the applicable Creative Commons License

response curve of net photosynthetic rate examines short-term (or 'instantaneous') temperature responses, while day: night temperatures (low 18:13°C, moderate 26:21°C, high 34:29°C) treatments for growing plants represent medium-term temperature acclimation. The performance of populations to temperature-related bioclimatic variables at genotypic origins reflects the long-term thermal adaptation. Our hypotheses are: (1) Thermal acclimation to growth temperature will have a greater impact on overall photosynthetic temperature performance than local adaptation to climate of origin; (2) Phenotypic plasticity in photosynthetic performance will exhibit positive latitudinal patterns, with genotypes from higher latitudes exhibiting greater acclimation plasticity and faster adjustment of photosynthetic processes for optimal performance.

2 | Materials and Methods

2.1 | Preparation and Temperature Treatments of *Phragmites australis* Genotypes

P. australis (Cav.) Trin. ex. Steud. (common reed), a widespread wetland plant, displays high intraspecific diversity and phenotypic plasticity, enabling it to adapt to diverse environmental conditions (Eller et al. 2017). Its broad ecological amplitude and adaptability make it an ideal model for studying plant responses to global change. Diverse lineages of *P. australis*, subject to varying selective pressures from global change, show strong geographical patterns of intraspecific variation (Saltonstall 2002; Lambertini et al. 2012; Ren et al. 2020). Here, 18 genotypes, covering three main phylogeographical groups of *P. australis*, European (EU), North American (NA) and Chinese (CN) and a latitudinal range from 36° to 56° N, were chosen to examine intraspecific variation in thermal acclimation (Table 1).

Genotypes were sourced from a common garden of live *P. australis* at Aarhus University, Denmark (56° 13′ N; 10° 07′ E). Clones (genetically identical replicates) were produced by layering of shoots horizontally in shallow water for 4 weeks until adventitious shoots reached 15–20 cm and had developed roots. Stems were then cut at nodes, and 3–4 clones were planted in 3.5 L pots with 1:1 sand and peat mixture. Each potted replicate received 500 mL of nutrient solution weekly (Pioner NPK macro 19-2-15 + Mg GRØN, Horticoop Scandinavia: 11.9 mg L^{-1} NO_3-N, 7.4 mg L^{-1} NH_4-N, 2.3 mg L^{-1} P, 15.4 mg L^{-1} K, 3 mg L^{-1} Mg, 3.9 mg L^{-1} S and Pioner Mikro + Fe, in μM: 0.02 B, 2.2 Cu, 24 Fe, 9.1 Mn, 0.5 Mo and 2.8 Zn, plus additional iron: 0.6 mM Fe(II)SO_4).

Plants were placed in three indoor growth cabinets (BIO 1000-2000S, Weiss Umwelttechnik GmbH, Lindensruth, Germany) with a 14:10 h light: dark cycle, 65:50% relative air humidity (day: night) and approximately 400 μmol m^{-2} s^{-1} (PAR) daytime irradiance. After a 2-week acclimatisation at 25:20°C (day: night), temperatures were adjusted to 18:13°C (low), 26:21°C (moderate) and 34:29°C (high) based on the average temperatures of the warmest month of the genotypes'

TABLE 1 | Geographical origin of the genotypes of *Phragmites australis* used in this study.

Genotype	Latitude of origin (°)	Longitude of origin (°)	Country of collection (phylogeographical group)	MAT (°C)	Temperature seasonality (C of V)	Temperature annual range (°C)
FE2017CN	37.05	118.07	China (CN)	13.369	0.015	19.523
FE2018CN	37.05	118.07	China (CN)	13.369	0.026	33.890
FE2023CN	36.46	120.68	China (CN)	12.309	0.028	33.797
FE2024CN	41.09	122.06	China (CN)	9.267	0.029	36.458
FE2025CN	41.09	122.06	China (CN)	9.267	0.033	36.097
FE2028CN	41.21	122.03	China (CN)	9.254	0.037	41.184
EU60GB	56.46	−3.05	Great Britain (EU)	8.047	0.019	21.500
EU164IE	53.43	7.95	Ireland (EU)	8.698	0.025	29.790
EU172SL	46.06	14.51	Slovenia (EU)	10.063	0.029	34.877
EU207IT	45.68	9.77	Italy (EU)	10.992	0.024	29.103
EU620CZ	48.65	14.37	Czech Republic (EU)	6.786	0.024	28.603
EU801SW	47.33	8.53	Switzerland (EU)	8.658	0.022	24.984
NAint99US	36.27	−77.59	United States (UA)	15.089	0.035	39.877
NAint115US	38.77	−76.08	United States (UA)	13.379	0.035	39.877
NAint116US	47.13	−119.28	United States (UA)	10.446	0.033	33.926
NAint129CA	43.67	−79.42	Canada (UA)	7.915	0.041	43.158
NAint152US	45.57	−73.85	United States (UA)	6.116	0.041	43.158
NAint180US	39.58	−75.71	United States (UA)	12.336	0.041	43.536

Note: Temperature seasonality is measured using the standard deviation of monthly mean temperatures. Temperature annual range (°C) = Max temperature of warmest week (°C) − Min temperature of coldest week (°C).

13653040, 2025, 7, Downloaded from https://onlinelibrary.wiley.com/doi/10.1111/pce.15452 by East China Normal University, Wiley Online Library on [03/06/2025]. See the Terms and Conditions (https://onlinelibrary.wiley.com/terms-and-conditions) on Wiley Online Library for rules of use; OA articles are governed by the applicable Creative Commons License

original habitat, to cover a realistic and broad growth temperature regime. Each genotype had two replicated pots (3–4 replicated clones in each 3.5 L pot) in each chamber, and plants were kept moist throughout the 60-day study. To mitigate edge effects, pots holding the plants were rotated within the growth chambers weekly.

2.2 | Functional Growth Traits

Functional growth traits were monitored by measuring the number and tallest shoot height per pot weekly. Shoot elongation rate (SER, cm d^{-1}) was assessed by measuring the height of all shoots at the start and end of the experiment to calculate cumulative height gain. Shoot production rate (SPR, g d^{-1}) was determined as the daily productivity of shoots over the experimental period. Post-experiment, plants were harvested, separated into leaves, stems, roots and rhizomes and oven-dried at 80°C to constant weight. Biomass allocation for each fraction was calculated as its ratio to total dry mass, and the root: shoot ratio was determined as the biomass ratio of root and rhizome to stem and leaf. All measurements above had at least three replicates per treatment per genotype.

2.3 | Light and CO_2-Response Curves

Following 45 days of growth under the three temperature regimes, the gas-exchange characteristics of three replicated fully developed leaves per treatment per genotype. We tried to make sure that measurements were carried out on the same leaf with a mark. Unless there is accidental damage, replace the adjacent intact leaf. Gas exchange responses to light (A/I curves) and intercellular CO_2 concentration (A/C_i curves) were measured after 4 weeks of temperature treatment, respectively, using an infra-red gas analyser (IRGA; LI-6400XT, Li-Cor, Lincoln, NE, USA). The flow rate was kept stable at 500 μmol mol^{-1} with stable VPD and humidity (65%) maintained by manually controlling airflow through the device's desiccant tube.

A/I curves were generated at a constant CO_2-concentration of 400 ppm. The light intensity was adjusted to 1500, 1200, 800, 450, 100, 50 and 0 μmol m^{-2} s^{-1} using a red/blue LED light source. The light intensities were changed and gas exchanged rates were logged by prompting an auto-program, starting after stabilisation of the photosynthetic rate at 1500 μmol m^{-2} s^{-1}. The cuvette temperature was set to ambient temperature, and the CO_2 concentration was 400 ppm. During measurements at highest light intensities (A_{max}; μmol m^{-2} s^{-1}), the transpiration rate (E; mmol m^{-2} s^{-1}) and stomatal conductance (g_s; mol m^{-2} s^{-1}) and intercellular CO_2 concentration (C_i; μmol μmol $^{-1}$) were recorded. A/I curves were modelled using:

$$A_n = \frac{\Phi \cdot I + A_{max} - \sqrt{(\Phi \cdot I + A_{max})^2 - 4\Theta \cdot \Phi \cdot I \cdot A_{max}}}{2\Theta} - R_d \quad (1)$$

fitting to the non-rectangular hyperbola by Prioul and Chartier (1977) in a non-linear regression, where Θ (dimensionless) determines the curvature of the function, I is the set light intensity. The model yields the light-saturated photosynthesis rate (A_{max}), the dark respiration rate (R_d) and the photosynthetic quantum yield (Φ). The light compensation point (I_c) was calculated according to this curve where photosynthetic rate matches the cellular respiration rate. The light saturation point (I_k) was the light intensity estimated when photosynthetic rate reached 90% of the maximum net photosynthetic rate.

A/C_i curves were also auto-logged with the LI-6400XT, with a minimum waiting time of 60 s and a maximum waiting time of 240 s. After stabilisation of the photosynthetic rate at an ambient CO_2 concentration of 400 ppm in the reference air, the concentration was changed to 250, 100, 50, 400, 400, 400, 600, 700, 800 and 1000 ppm CO_2 accordingly. CO_2 was supplied from a 12 g CO_2 cartridge mounted in the instrument, with a stable light intensity of 1500 μmol m^{-2} s^{-1} and at the daytime growth temperature. The fitting was done using the Farquhar et al. (1980) models (FvCB) with the fitaci() function in the R-package '*plantecophys*' (Duursma 2015). The models yield the maximum electron transport rate (J_{max}, μmol m^{-2} s^{-1}), the maximum carboxylation rate of Rubisco (V_{cmax}, μmol m^{-2} s^{-1}) and rate of triose phosphate utilisation (TPU, μmol m^{-2} s^{-1}).

$$A_n = \frac{A_c + A_j - \sqrt{(A_c + A_j)^2 - 4\Theta \cdot A_c \cdot A_j}}{2\Theta} - R_d \quad (2)$$

where A_c is the gross photosynthesis rate when Rubisco activity is limiting, A_j when RuBP-regeneration is limiting, R_d is the rate of mitochondrial respiration and Θ (dimensionless) determines the curvature of the function. According to Farquhar et al. (1980), A_n could be modelled as the hyperbolic minimum of A_c and A_j, A_n= min (A_c, A_j) − R_d. The temperature dependence of the CO_2-compensation point (Γ^*, μmol mol^{-1}) was calculated according to Bernacchi et al. (2001) with adjustments for photorespiration. When $A = R_d$, where the rate of CO_2 uptake by RuBP carboxylationequals the rate of CO_2 release by RuBP oxygenation. At this point, the CO_2 concentration within the chloroplast, termed the CO_2 compensation point in photosynthesis, is denoted as Γ^*:

$$\Gamma^* = \frac{0.5O}{\tau} \quad (3)$$

where τ is the Rubisco specificity factor = K_c V_{omax}/(K_o V_{cmax}) (Harley and Sharkey 1991). K_c and K_o are the Michaelis–Menten constants for CO_2 and O_2, respectively; V_{omax} is the maximum rate of oxygenation (Farquhar et al. 1980).

2.4 | Photorespiration and Photosynthetic Temperature Response Curves

After 5 weeks of experimental treatment, photosynthetic temperature response curves were measured using an infra-red gas analyser (IRGA; LI-6400XT, Li-Cor, Lincoln, NE, USA). The measurements were conducted on three replicated fully developed leaves per treatment and genotype. The flow rate was kept stable at 500 μmol mol^{-1} with stable humidity (65%), ensured by manually controlling airflow through the device's desiccant

13653040, 2025, 7, Downloaded from https://onlinelibrary.wiley.com/doi/10.1111/pce.15452 by East China Normal University, Wiley Online Library on [03/06/2025]. See the Terms and Conditions (https://onlinelibrary.wiley.com/terms-and-conditions) on Wiley Online Library for rules of use; OA articles are governed by the applicable Creative Commons License

tube. Measurements were taken at a stable irradiance of 1500 μmol m^{-2} s^{-1}. The IRGA's limited temperature adjustment capacity necessitated changing the growth chamber temperature for respective measurement, while the curves were made. The measurements were taken at intervals of 15°C, 22°C, 28°C, 34°C, 41°C. Five readings were recorded at each temperature for each leaf sample. After each temperature adjustment, a 30-min waiting period was observed to allow the plants to acclimate to the new temperature before measurements were taken. Temperature response curves were conducted at ambient O_2 air concentration (21%) and at a 2% O_2 concentration to estimate temperature response with suppressed photorespiration. The lower O_2 concentration was achieved by mixing technical atmospheric air and N_2 into the reference airstream using a gas mixer (ADC, Hoddesdon, Great Britain). The reference CO_2 concentration was maintained at 400 ppm. The model of temperature response curves was fitted with a quadratic equation (Battaglia et al. 1996; Gunderson et al. 2010; Kumarathunge et al. 2019), expressed as:

$$A_n = A_{net} - b(T - T_{opt})^2 \quad (4)$$

where T_{opt} was the optimum temperature, A_{net} is the net photosynthetic rate at T_{opt}, A_n is the net photosynthetic rate at a given leaf temperature T (°C) and the parameter b (unitless) describes the degree of curvature of the parabola. A larger b value reflects a narrower range of optimum temperatures, while a smaller b value results in a broader curve (Gunderson et al. 2010).

The relative difference between thermal optimum at 2% and 21% O_2 concentration is defined as $R_{Topt} = T_{opt2}/T_{opt21}$. The relative difference between net photosynthetic rate at thermal optimum in 2% and 21% O_2 concentration is defined as $R_{Anet} = A_{net2}/A_{net21}$. O_2 sensitivity of photosynthesis is defined as $OS(A) = (A_{net2} - A_{net21})/A_{net2}$; CO_2 sensitivity of photosynthesis is defined as $CS(A) = (A_{air} - A_{sat})/A_{sat}$ (Sage et al. 1990; Sage and Kubien 2007; Busch and Sage 2017), where A_{net21} and A_{net2} are net CO_2 uptake at 21% and 2% O_2 levels where photorespiration is nil, respectively, and A_{air} and A_{sat} are net CO_2 uptake at an atmospheric ambient and saturating CO_2 levels, according to measurements for A/C_i curves.

2.5 | Phenotypic Plasticity

We used a simplified relative distance plasticity index ($RDPI_s$) to compare the adaptability of genotypes to varying environmental conditions by quantifying the phenotypic distances between pairwise individuals of each genotype grown under different environments. The $RDPI_s$ for each genotype (j) in every growth temperature (i) and the average of each measured parameter were calculated according to Valladares et al. (2007):

$$RDPI_s = \Sigma(dij \rightarrow i'j'/(xi'j' + xij))/n \quad (5)$$

where n is the number of individual distances. The index ranges from 0 (not plastic) to 1 (maximal plasticity).

2.6 | Statistical Data Analysis

All data were analysed in R version 4.1.1 (R Core Team 2021). The mean values of each of the three replicated leaves per genotype per treatment were used to generate the curves and all data analyses.

To test the photosynthetic temperature responses of *P. australis* differ among phylogeographical groups indicating local adaptation and temperature treatments indicating acclimation, we fitted each measured trait with (generalised) linear mixed models using 'Phylogeographic group', 'Temperature' and their interaction as fixed factors and 'Genotype' as a random effect to represent unexplained variance among genotypes (Zuur et al. 2009). We checked for overdispersion and underdispersion, using Poisson distribution for J_{max}, I_k and A_{max}, negative binomial distribution for V_{cmax}, CO_2 compensation point and C_i and normal distribution for other traits (package '*nlme*' and '*lme4*') (Pinheiro et al. 2020; Bates et al. 2015). Quantile–quantile plots were drawn for model validation. The numerator degrees of freedom (numDF), denominator degrees of freedom (denDF), F values and p values for Wald tests for fitted models were assessed. To test the goodness of fit for each model, marginal R^2 (variance explained by fixed factors alone in mixed models) and conditional R^2 (variance explained by both fixed and random factors in mixed models) were computed (package '*MuMIn*') (Bartoń 2020). Two-way analysis of variance for individual traits was conducted using *Wald chi-square* tests (package 'car'), with six genotypes as replicates within each phylogeographical groups and temperatures (Fox and Weisberg 2019). Two-way analysis of variance of 'Temperature', 'Oxygen' and their interactions (eighteen genotypes as replicates) for optimum temperature, net photosynthetic rate at thermal optimum and parameter b were conducted to assess the effect of temperature and O_2 concentration on T_{opt}. In addition, we conducted linear regressions to compare how T_{opt} of *P. australis* from different phylogeographical groups responded to increasing growth temperature at ambient O_2 air concentration and at a 2% O_2 concentration, respectively. The equations for the relationship ($n = 18$), along with the R^2 values and significance levels, are provided. The relationships between O_2 sensitivity of the mean value of six replicated genotypes and leaf temperature were modelled using quadratic linear regressions for each phylogeographical group and growth temperature.

To compare the relative contribution of adaption and acclimation to the overall photosynthetic temperature responses of *P. australis*, we performed principal component analyses on all measured traits using the '*factoextra*' and '*factoMinR*' packages (Husson et al. 2020, Kassambara and Mundt 2020). Mean annual temperature (MAT,°C), temperature seasonality (C of V) and temperature annual range (°C) were obtained from the bioclimatic variables (bio01, bio04 and bio07) in the data set CliMond Archive (V1.2) (Kriticos et al. 2012). To assess the effects of temperature conditions at genotypic origins on T_{opt}, we conducted linear regressions between T_{opt} of all genotypes and temperature variables at genotypic origins (MAT, temperature seasonality and temperature annual range), respectively. Where necessary, log-transformed and rechecked for normal distribution.

13653040, 2025, 7, Downloaded from https://onlinelibrary.wiley.com/doi/10.1111/pce.15452 by East China Normal University, Wiley Online Library on [03/06/2025]. See the Terms and Conditions (https://onlinelibrary.wiley.com/terms-and-conditions) on Wiley Online Library for rules of use; OA articles are governed by the applicable Creative Commons License

To test the hypothesis that the RDPIs across varying growth temperature ($n = 18$ genotypes) or O_2 concentration ($n = 54$ genotypes×temperature treatments) of *P. australis* physiological traits change along latitudinal gradients, we conducted linear mixed models with 'Latitude' as an independent factor for each trait. Linear regression and quadratic regression equations were compared according based on the Akaike Information Criterion for model optimisation. Quantile–quantile plots were used for model validation. The equations for the relationship, along with the R^2 values and significance levels, are provided.

3 | Results

3.1 | Short-Term Temperature Response Curves

As leaf temperature increased, the net photosynthetic rate of all phylogeographical groups showed a trend of first increasing rapidly and then slowly decreasing (Figure S1a). The thermal optimum for photosynthesis (T_{opt}) increased by 0.30°C, 0.49°C and 0.23°C in the CN, EU and US groups per°C increase in growth temperature under ambient air conditions, and by 0.28°C, 0.79°C and 0.34°C, respectively, at 2% O_2 concentration (Figure 1a).

O_2 concentration significantly affected T_{opt} and A_{net}, both of which were higher in 2% O_2 concentration treatment than in the ambient air O_2 concentration, with an average shift in T_{opt} of about 2.5 °C and an increase in A_{net} at T_{opt} of over 10 μmol m^{-2} s^{-1} (Figure S1b). On average, the shift in T_{opt} was 1.9°C, 1.9°C and 3.9°C for the low, moderate and high growth temperature, respectively, and the shift in T_{opt} was 1.0°C, 4.5°C and 2.2°C for the CN, EU and US groups, respectively. Correspondingly, the average shift in A_{net} at T_{opt} was approximately 9, 12 and 9 μmol m^{-2} s^{-1} for the same groups. Therefore, the relative difference in T_{opt} between 2% and 21% O_2 concentration (R_{Topt}) for the EU group was highest than the US and CN groups (Figure 1b). In

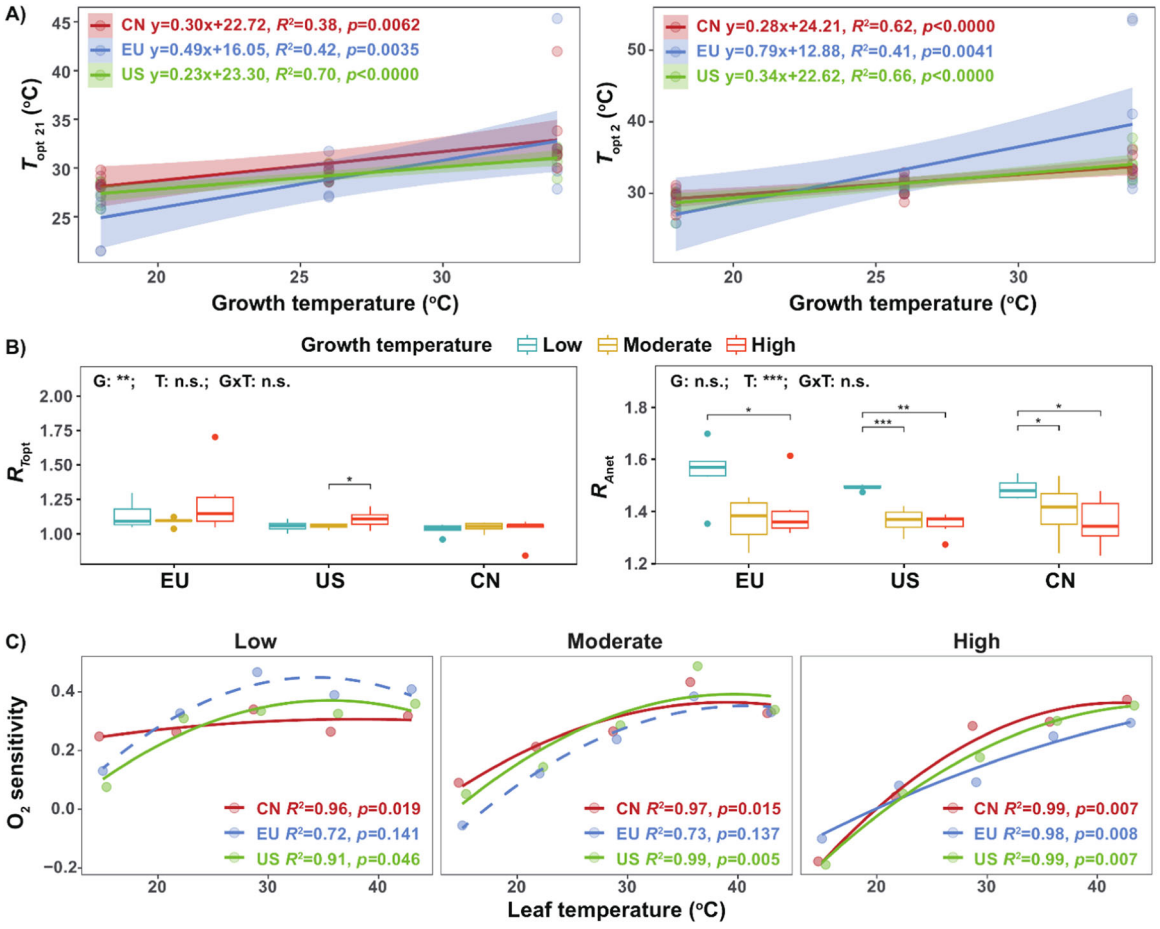


FIGURE 1 | (a) Optimum temperature for photosynthesis at ambient oxygen air concentration (T_{opt21}, °C, (a)) and at a 2% oxygen concentration (T_{opt2}, °C, (b)) against growth temperature (°C) for phylogeographical groups of *Phragmites australis* from China (CN), Europe (EU) and United States (US). The equations for the relationship ($n = 18$), along with the R^2 and p values are provided. (b) Variation of the relative difference in optimal temperature (R_{Topt}) and net photosynthetic rate at optimum temperature (R_{Anet}) between 2% and 21% O_2 concentration in *Phragmites australis* among phylogeographical groups of US, EU and CN grown at low, moderate and high temperatures. Significance among phylogeographical groups (G; numDF = 2, denDF = 15), growth temperature (T; numDF = 2, denDF = 30) and their interactions (GxT; numDF = 4, denDF = 30) is shown according to ANOVA analysis. Pairwise comparisons between growth temperature within each phylogeographical group using emmeans with Bonferroni adjustment for p-values (*** < 0.001; ** 0.01; * ≤ 0.05). (c) The effects of leaf temperature variation ($n = 5$) on the average O_2 sensitivity of photosynthesis (n = 6 genotypes within each phylogeographical group and temperature treatments) in *P. australis* from CN, EU and US phylogeographical groups grown at low, moderate and high temperatures. R^2 and p values are provided.

13653040, 2025, 7, Downloaded from https://onlinelibrary.wiley.com/doi/10.1111/pce.15452 by East China Normal University, Wiley Online Library on [03/06/2025]. See the Terms and Conditions (https://onlinelibrary.wiley.com/terms-and-conditions) on Wiley Online Library for rules of use; OA articles are governed by the applicable Creative Commons License

addition, the relative difference in net photosynthetic rate at thermal optimum (R_{Anet}) between 2% and 21% O_2 concentration significantly decreased as temperature increased (Figure 1b).

The sensitivity of A to a change in O_2, OS(A), varied significantly among growth temperatures, showing higher sensitivity in the low growth temperature treatment (Table S1 and Figure 1c). In response to increasing leaf temperature, OS(A) consistently exhibited a trend of initially increasing and then leveling off at warmer temperatures. The upward trend was most pronounced at high growth temperatures (Figure 1c). The responses of OS(A) for the CN group to increasing leaf temperature was weaker compared to the other two groups under low-temperature treatment (Figure 1c).

3.2 | Medium-Term Acclimation to Growth Temperature and Long-Term Adaptation to the Climates at Genotypic Origins

Medium-term growth temperature significantly affected all functional growth traits of *P. australis*, including tissue biomass, biomass allocation, root: shoot ratio, shoot production rate and shoot elongation rate (SER) (Table S1). Higher temperature remarkably increased the dry mass of all plant tissues, but decreased rhizome and root allocation, resulting in a lower root: shoot ratio at high temperatures (Figures 2 and S2). SPR and SER also increased with rising temperature (Figure 2). In addition, the biomass of leaves, stems and rhizomes, as well as the biomass allocation of stems and rhizomes and SER, were significantly different among phylogeographical groups (Table S1 and Figure 2), indicating the adaptation to original climates. The biomass responses of the CN group to increasing temperatures were distinct from those of the EU and US groups, showing a continuously increasing trend for both aboveground and belowground biomass (Figure S3). The CN group also exhibited the highest average SPR and SER compared to the EU and US groups (Figure 2).

Most light-response photosynthetic traits, such as A_{max}, g_s, E, I_k, I_c and R_d, generally had positive responses to rising growth temperature, except for C_i and Φ (Figure 3 and Table S1). According to the light-response curves, A_{max}, g_s, I_k showed significant differences among phylogeographical groups, with the CN group typically having higher values than the EU and US groups (Table S1 and Figure 3b).

From the CO_2-response of photosynthesis, V_{cmax}, J_{max}: V_{cmax}, TPU, Γ^* and CO_2-saturated photosynthesis rate (A) were significantly different among growth temperatures (Table S1 and Figure 4). TPU, Γ^* and CO_2-saturated A of *P. australis* increased with rising temperature (Figure 4b). Additionally, the sensitivity of A to CO_2 changes, CS(A), also increased with growth temperatures, although the change was not statistically significant (Figure 4b). V_{cmax}, TPU, Γ^* and CO_2-saturated A were significantly different among phylogeographical groups (Table S1 and Figure 4b) was lower in CN groups across all temperatures, but V_{cmax} for CN group was higher in low-temperature treatment. J_{max}: V_{cmax} of different phylogeographical groups responded differently to varying temperatures (Figure 4). The sensitivity of A to CO_2 changes, CS(A), for the CN and US groups increased with growth temperatures, while it decreased for the EU group (Figure 4b).

According to the PCA analysis (Figure S3 and Table S2) medium-term acclimation to growth temperature had the greater influences on *P. australis* performance than long-term adaptation, as high, moderate and low temperatures groups are

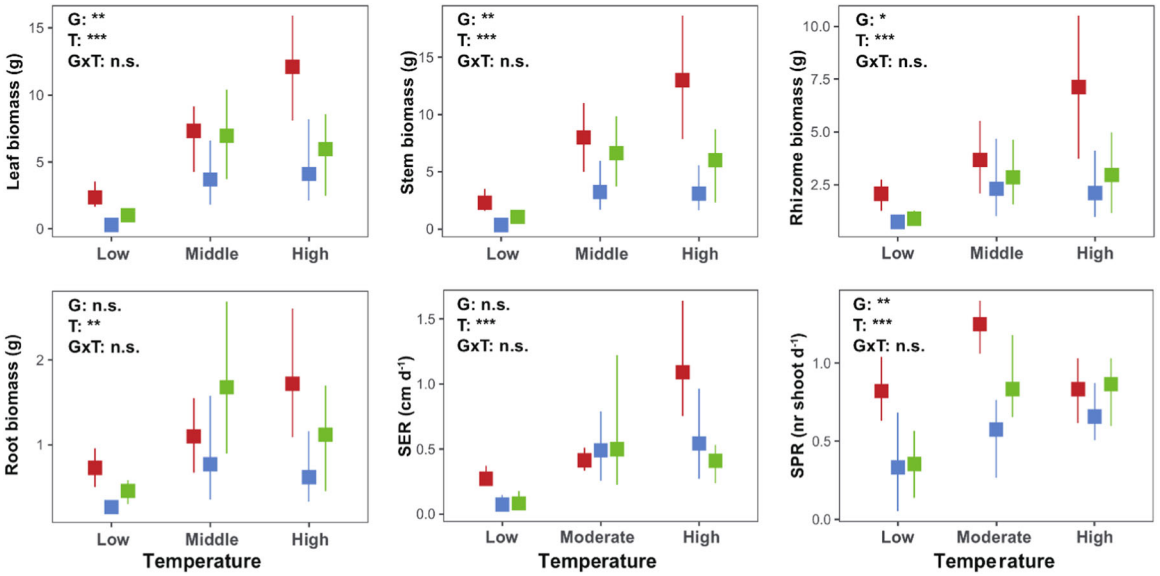


FIGURE 2 | Comparison of growth traits in *Phragmites australis* from phylogeographical groups of Europe (EU), North America (US) and China (CN) grown at low, moderate and high temperatures and their interactions. SPR, shoot production rate (g day^{-1}); SER, shoot elongation rate (cm day^{-1}). The mean values of six genotypes within each phylogeographical group and temperature treatments, as well as associated 95% confidence intervals, are shown. Overlapping intervals indicate no significant difference between phylogeographical groups or temperature treatments. Significance levels among phylogeographical groups (G; numDF = 2, denDF = 15), growth temperature (T; numDF = 2, denDF = 30) and their interactions (GxT; numDF = 4, denDF = 30) are shown according to ANOVA analysis. Significant levels: ***< 0.001; **< 0.01. [Color figure can be viewed at wileyonlinelibrary.com]

13653040, 2025, 7, Downloaded from https://onlinelibrary.wiley.com/doi/10.1111/pce.15452 by East China Normal University, Wiley Online Library on [03/06/2025]. See the Terms and Conditions (https://onlinelibrary.wiley.com/terms-and-conditions) on Wiley Online Library for rules of use; OA articles are governed by the applicable Creative Commons License

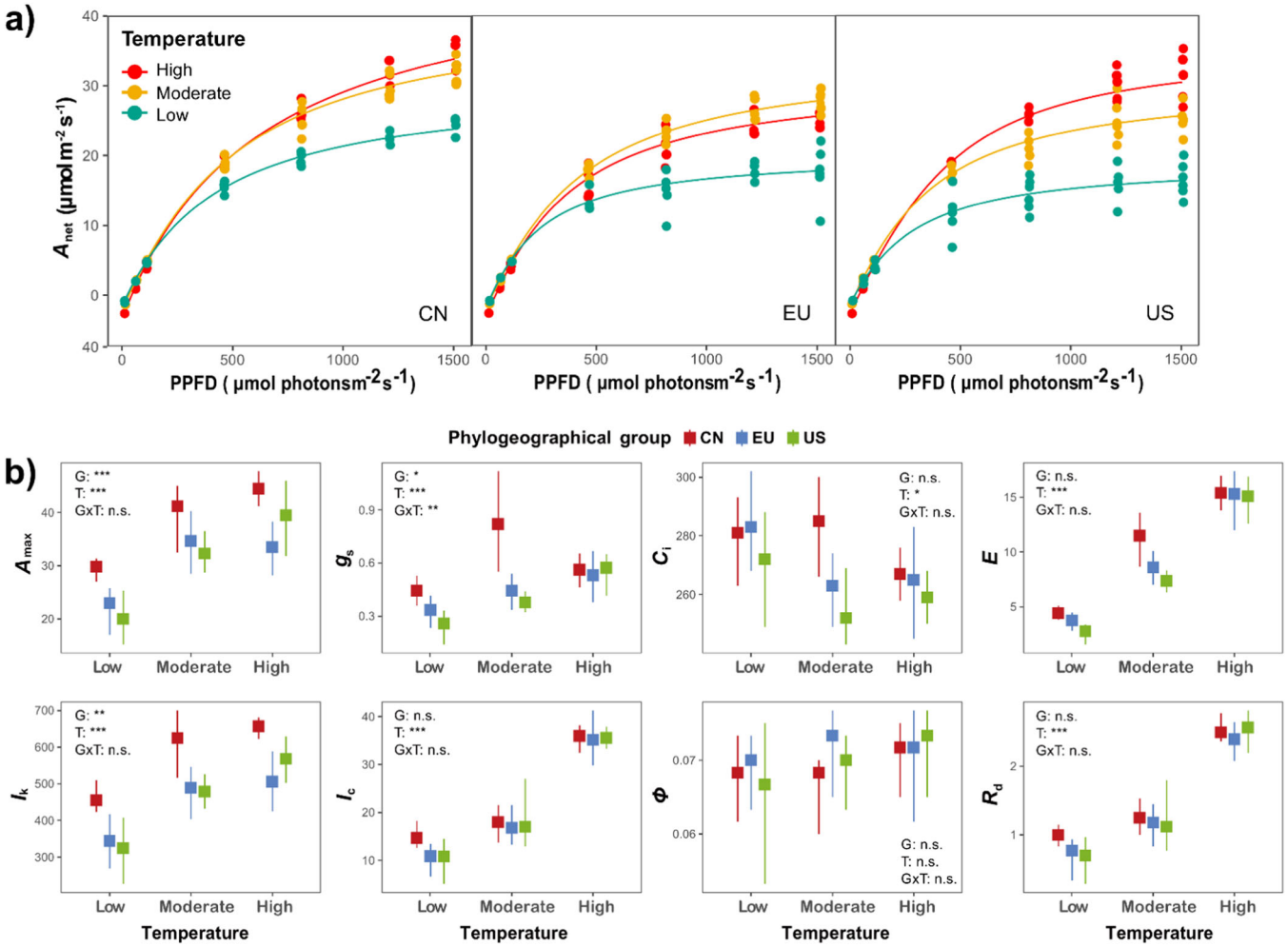


FIGURE 3 | (a) Average light response curve of net photosynthesis rate (A_{net}, μmol m^{-2} s^{-1}; $n = 6$ genotypes within each phylogeographical group and temperature treatments) in *Phragmites australis* from phylogeographical groups of EU, US and CN grown at low, moderate and high temperatures. (b) Comparison of traits related to the light response curve of net photosynthesis rate in *Phragmites australis* from phylogeographical groups of Europe (EU), North America (US) and China (CN) grown at low, moderate and high temperatures. A_{max}, highest light intensities (μmol m^{-2} s^{-1}); g_s, stomatal conductance (mol m^{-2} s^{-1}); C_i, intercellular CO_2 concentration (μmol μmol^{-1}); E, the transpiration rate (mmol m^{-2} s^{-1}); I_k, the light saturation point; I_c, the light compensation point; Φ, the photosynthetic quantum yield; R_d, the dark respiration rate (μmol m^{-2} s^{-1}). Mean values of six genotypes within each phylogeographical group and temperature treatments, and associated 95% confidence intervals are displayed. Overlapping intervals indicate no significant difference between phylogeographical groups or temperature treatments. Significance levels among phylogeographical groups (G; numDF = 2, denDF = 15), growth temperature (T; numDF = 2, denDF = 30) and their interactions (GxT; numDF = 4, denDF = 30) are shown according to ANOVA analysis. Significant levels: ***< 0.001; **< 0.01; *< 0.05. [Color figure can be viewed at wileyonlinelibrary.com]

aligned along PC1, while phylogeographical groups clustered together. In addition, we found T_{opt21} and T_{opt2} significantly responded to temperature seasonality (C of V) and temperature annual range (°C) at genotypic origins under low or high growth temperature treatment (Figure 5 and Table S3), indicating the interactive effects of midterm thermal acclimation and local adaptation to climate of origin.

3.3 | Phenotypic Plasticity Across Temperatures and Oxygen Concentrations

The relative distance plasticity indelative distance plasticity index (RDPIs) for varying growth temperatures in *P. australis* showed significantly latitudinal patterns in both growth and photosynthetic traits. Growth traits' RDPIs, including leaf biomass and allocation, rhizome allocation, root: shoot ratios and SPR, increased with higher latitudes at genetic origins, while RDPIs for Γ decreased (Figure 6). RDPIs of T_{opt} in 2% O_2 concentration and $R_{T\text{opt}}$ initially decreased and then increased with increasing latitudes. Moreover, RDPIs for varying O_2 concentrations in T_{opt} also significantly increased with higher latitudes at genetic origins (Figure 6 lower right corner with triangles).

4 | Discussion

4.1 | Thermal Optimum for Photosynthesis and the Effect of Oxygen Concentration

Global studies indicate that growth temperature is a key driver for T_{opt}, which found the mean rate of increase in T_{opt} was

13653040, 2025, 7, Downloaded from https://onlinelibrary.wiley.com/doi/10.1111/pce.15452 by East China Normal University, Wiley Online Library on [03/06/2025]. See the Terms and Conditions (https://onlinelibrary.wiley.com/terms-and-conditions) on Wiley Online Library for rules of use; OA articles are governed by the applicable Creative Commons License

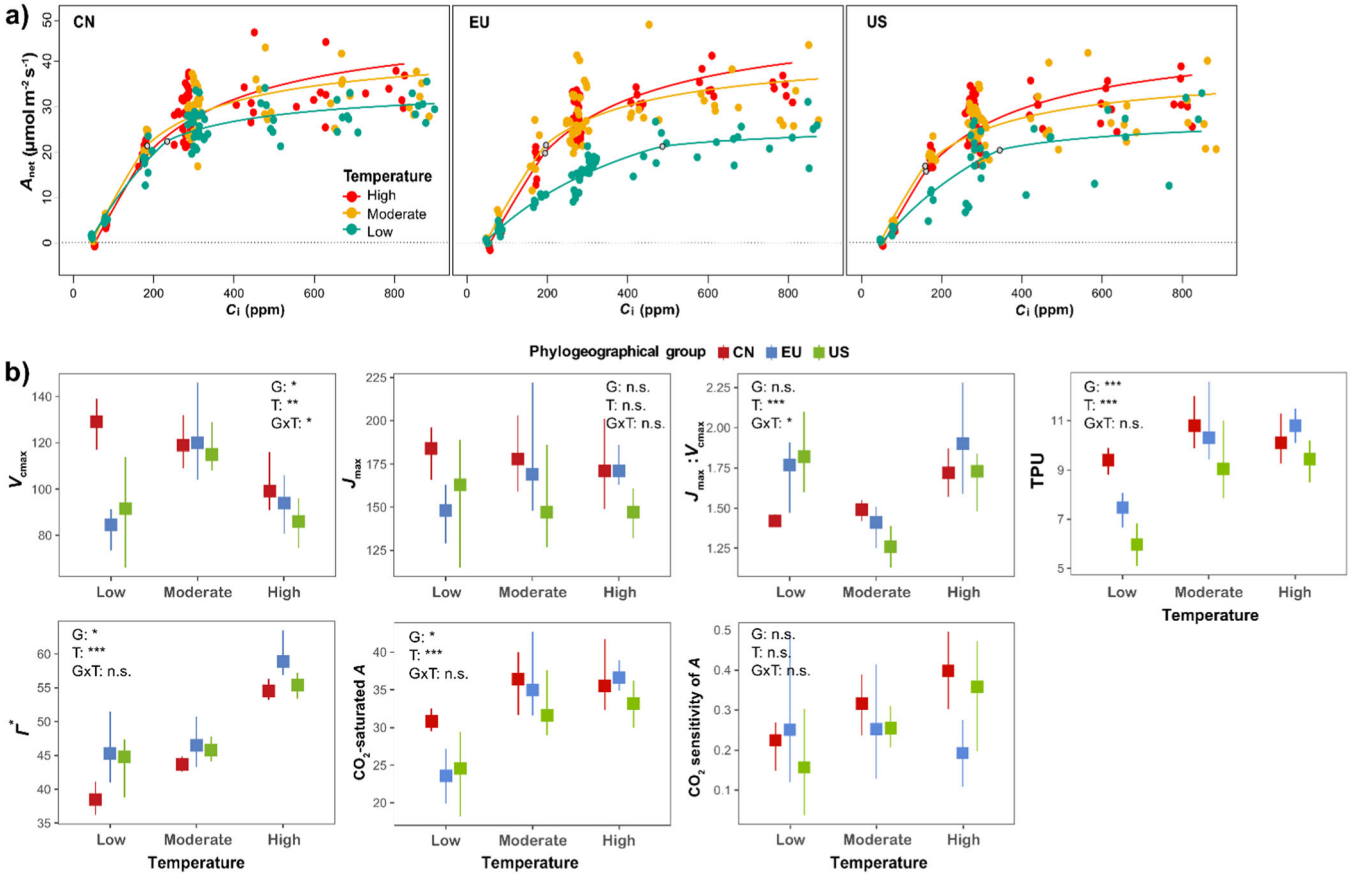


FIGURE 4 | (a) Average CO_2 response curve of net photosynthesis rate (A_{net}, μmol m^{-2} s^{-1}; $n = 6$ genotypes within each phylogeographical group and temperature treatments), fitted with the FvCB model, in *Phragmites australis* from phylogeographical groups of EU, US and CN grown at low, moderate and high temperatures. Hollow points indicate the intersection points between the A_c and A_j curves (i.e., the CO_2 assimilation rate at which the A/C_i curve switches between the Rubisco- and RuBP-limited curves). (b) Comparison of traits related to CO_2 response curve of net photosynthesis rate in *Phragmites australis* from phylogeographical groups of US, EU and CN grown at low, moderate and high temperatures. J_{max}, the maximum electron transport rate (μmol m^{-2} s^{-1}); V_{cmax}, the maximum carboxylation rate of Rubisco (μmol m^{-2} s^{-1}); TPU, rate of triose phosphate utilization (μmol m^{-2} s^{-1}); Γ^*, the temperature dependence of the CO_2-compensation point (μmol mol^{-1}), CO_2-saturated A (μmol m^{-2} s^{-1}). Mean values of six genotypes within each phylogeographical group and temperature treatments, and associated 95% confidence intervals are shown. Overlapping intervals indicate no significant difference between phylogeographical groups or temperature treatments. Significance levels among phylogeographical groups (G; numDF = 2, denDF = 15), growth temperature (T; numDF = 2, denDF = 30) and their interactions (GxT; numDF = 4, denDF = 30) are shown according to ANOVA analysis. Significant levels: ***< 0.001; **< 0.01; *< 0.05. [Color figure can be viewed at wileyonlinelibrary.com]

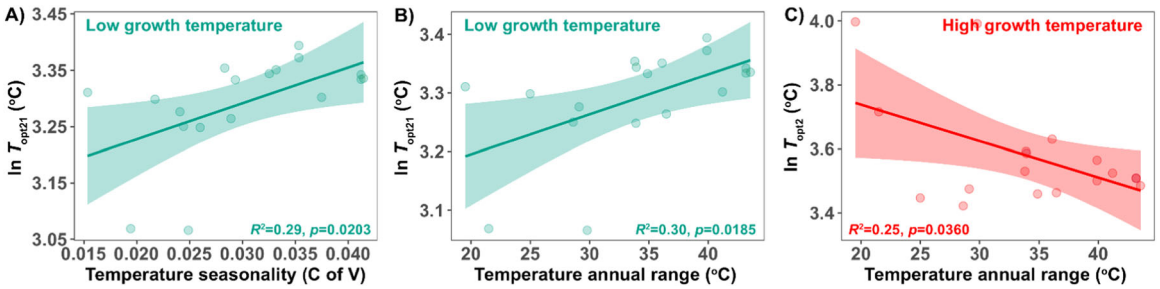


FIGURE 5 | Effects of temperature conditions at genotypic origins on T_{opt}. Only significant relationship provided. The relationship between ln T_{opt21} at 21% O_2 and temperature seasonality (C of V (a)) and temperature annual range (°C (b)) under low growth temperature conditions ($n = 18$ genotypes), as well as the relationship between T_{opt2} at 2% O_2 and temperature annual range (°C (c)) under high growth temperature ($n = 18$ genotypes). The R^2 and p values were provided. The shaded areas represent the 95% confidence intervals for the regression lines. [Color figure can be viewed at wileyonlinelibrary.com]

13653040, 2025, 7, Downloaded from https://onlinelibrary.wiley.com/doi/10.1111/pce.15452 by East China Normal University, Wiley Online Library on [03/06/2025]. See the Terms and Conditions (https://onlinelibrary.wiley.com/terms-and-conditions) on Wiley Online Library for rules of use; OA articles are governed by the applicable Creative Commons License

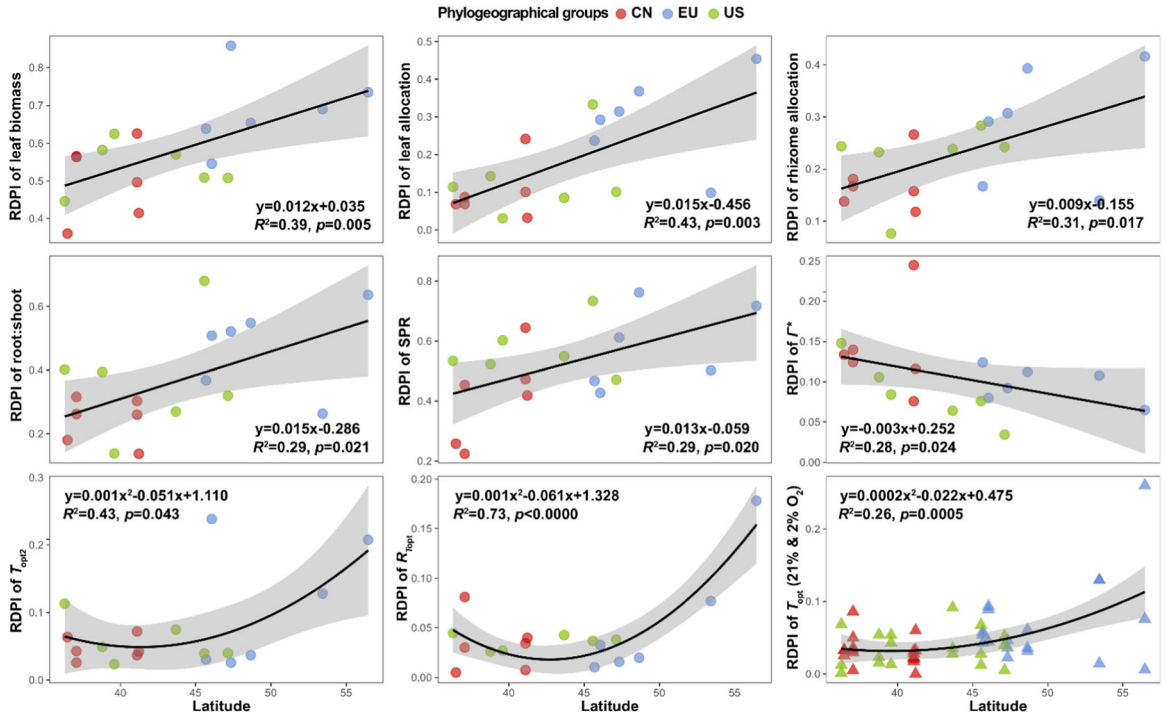


FIGURE 6 | Significant correlation ($p < 0.05$) between the relative distance plasticity index (RDPI) of traits and latitudes at genotypic origins in *Phragmites australis*, including the plasticity to varying growth temperature (circles; $n = 18$ genotypes) and plasticity to varying O_2 concentration (21% and 2%, triangles; $n = 54$ genotypes×temperature). Grey shadings represent 95% confidence intervals. Only significant correlations are shown. [Color figure can be viewed at wileyonlinelibrary.com]

about 0.62°C (Kumarathunge et al. 2019), 0.44°C and 0.33°C (Kattge and Knorr 2007) per °C increase in growth temperature. In our study, the average rate of T_{opt} increase was approximately 0.41°C per °C rise in growth temperature, including both O_2 concentrations. This variation may be attributed to differences in measurement conditions, as the data set encompassed measurements across CO_2 concentrations ranging from 40 to 2000 ppm, without accounting for O_2 concentrations.

In C_3 plants like *P. australis*, photorespiration can inhibit net photosynthetic assimilation when the enzyme Rubisco reacts with O_2 instead of CO_2 (Hesketh 1967). About 25% of the gross CO_2 fixation rate may be released by photorespiration, which typically increases with warming (Sharkey 1988; Walker et al. 2013). In our study, there was an average shift in thermal optimum above about 2.5°C and an increase in A_{net} at T_{opt} of about 10 μmol m^{-2} s^{-1} when suppressing photorespiration (Figure S1). Reducing O_2 concentration favours carboxylation over oxygenation by Rubisco, thereby increasing the efficiency of photosynthesis and the thermal optimum for photosynthesis in high-temperature environments (Wingler et al. 2000). We also found that the average shift in R_{Topt} of *P. australis* from all phylogeographical groups increased with rising growth temperature, while R_{Anet} decreased with rising growth temperature, showing the increasing the efficiency of photosynthesis and the diminishing relative advantage of reduced photorespiration in a low-O_2 environment at higher temperatures (Figure 1b). A previous study also found plants acclimate by adjusting their photosynthetic machinery, reducing the sensitivity of A_{net} to changes in O_2 concentration when growth temperature rises (Sage and Kubien 2007).

Additionally, the O_2 sensitivity of photosynthesis was stable and higher grown in low temperatures, while pronounced increased with increasing leaf temperature grown in high temperatures (Figure 1c), indicating plants grown in low growth temperatures had always lower photosynthetic efficiency, while plants grown in high-temperature environments had greater photosynthetic efficiency when leaf temperature is low and might experience greater fluctuations in photosynthetic efficiency to changing leaf temperature. Possible reasons include increased CO_2 solubility, reduced metabolic rates, higher Rubisco oxygen affinity, lower photorespiration compensation point and adaptations to cooler environments, all contributing to high sensitivity of the carboxylation-oxygenation balance to changes in O_2 concentration (Busch and Sage 2017). Additionally, the CN group's O_2 sensitivity response to increasing leaf temperature was weaker at low temperatures, while the EU group's response was lower at high temperatures, indicating their different physiological strategies to medium-term temperature changes due to long-term evolutionary adaptation to temperatures at genotypic origins.

4.2 | The Trends in Photosynthetic Response in Relation to Growth Temperature and Phylogeographical Groups' Thermal Environment

Phragmites australis exhibits a series of photosynthetic and growth responses, regulating plant acclimation to growth temperature. Across all phylogeographical groups, biomass components (leaf, stem, root and rhizome) generally increased with rising temperatures (Figure 2), which can attribute to enhanced

13653040, 2025, 7, Downloaded from https://onlinelibrary.wiley.com/doi/10.1111/pce.15452 by East China Normal University, Wiley Online Library on [03/06/2025]. See the Terms and Conditions (https://onlinelibrary.wiley.com/terms-and-conditions) on Wiley Online Library for rules of use; OA articles are governed by the applicable Creative Commons License

photosynthesis, improved resource availability and thermal adaptation. This shift allocated more resources to aboveground parts under warming conditions (Figure S2), reflecting a functional balance between aboveground and belowground resources in response to climate change (Ma et al. 2021).

According to the A/C_i curve, V_{cmax} decreased under high temperature for all groups. High temperatures may denature Rubisco, reduce its activity and favour oxygenation over carboxylation, increasing photorespiration and hence reducing the effective V_{cmax} for carbon fixation (Cen and Sage 2005). Previous studies have shown that declines in photosynthetic rate at high temperatures are usually due to Rubisco limitation rather than electron transport limitation (Busch and Sage 2017; Crous et al. 2022). The increase in J_{max}:V_{cmax} of at high temperatures in all phylogeographical groups suggests that *P. australis* uses a photosynthetic strategy with greater capacity for electron transport relative to Rubisco activity to adapt to high temperatures. Additionally, the decrease in J_{max}:V_{cmax} under moderate temperature for the EU and US groups may be in line with the least-cost optimality theory to maximise carbon uptake while minimising the associated costs (Smith and Keenan 2020).

Long-term local adaptation to climate of origin also significantly affected *P. australis* photosynthetic abilities, as evidenced by differences among phylogeographical groups. The CN group showed relatively higher A_{max}, g_s and I_k according to the photosynthetic light A/I curves (Figure 3b), indicating more stomatal opening, higher photosynthetic induction and more rapid activation of electron transport and Calvin-Benson cycle enzymes, such as Rubisco (Lambers and Oliveira 2019). The greater responses of V_{cmax} and J_{cmax} in the CN group, calculated by the A/C_i curves (Figure 4b), suggest higher mesophyll conductance, more activated Rubisco, or more resource allocation to photosynthetic processes, resulting in lower photorespiration costs due to adaptive genetic specification (Galmés et al. 2014). Furthermore, the kinetic properties of Rubisco, as indicated by Γ^*, revealed that the CN group exhibited the lowest CO_2 loss due to photorespiratory across all temperature treatments (von Caemmerer and Farquhar 1981; Sharkey 1988). This suggests that CN group populations may efficiently capture and utilise CO_2, potentially enhancing growth and photosynthesis, supported by their higher biomass (Figure 2).

Genotypes from the EU groups, adapted to cooler conditions over the long term, exhibited a more sensitive response in T_{opt} to increasing growth temperature. They showed the highest increases of 0.49°C and 0.79°C per °C rise in growth temperature under ambient air conditions and at 2% O_2 concentration, respectively (Figure 1a). In addition, the Rubisco enzyme in EU groups also seems to be more sensitive to variations in the ratio of CO_2 to O_2 concentration, with higher average R_{Topt} across all growth temperatures (Figure 1b). The reason may be that plants capable of better acclimation to low temperatures can allocate more nitrogen to RuBP regeneration, thus alleviating limitations (Yamori et al. 2014).

Our PCA analysis (Figure S3) indicates that medium-term acclimation to growth temperature has a stronger impact on overall photosynthetic performance in *P. australis* than long-term adaptation. Additionally, Figure 1a shows overlapping regression lines for each phylogeographical group, all demonstrating a consistent positive trend with increasing growth temperature. These align with Kumarathunge et al. (2019), who observed similar trends across 141 plant species excluding wetland species, suggesting that acclimation plays a more significant role in enhancing overall photosynthetic performance compared to long-term adaptations. However, under low and high growth temperature, the significant responses of T_{opt} to temperature seasonality and temperature annual range at genotypic origins (Figure 5), indicating that long-term local adaptation to climate of origin also strongly affected T_{opt} of *P. australis*. Previous studies also found that plants from thermally contrasting environments had considerable ability to maintain functional integrity at temperature extremes (Berry and Bjorkman 1980, Gunderson et al. 2010, Zhu et al. 2018).

4.3 | Phenotypic Plasticity in Photosynthetic Performance Along Geographical Gradients

In addition to local adaptation, phenotypic plasticity significantly influences plant growth and physiological traits in response to changing temperature environments (Yamori et al. 2010). Our study identified clinal patterns of phenotypic plasticity along latitude, suggesting that this plasticity, driven by natural selection, is heritable and favours plant functional traits that enhance success in changing environments. According to the CVH, populations at higher latitudes are expected to cope with broader environmental fluctuations due to pre-adaptation (Pither 2003; Pau et al. 2011). Populations from the margins of a species' distribution range typically have higher plasticity capacity and are better equipped to handle climate change and extremes (Valladares et al. 2014). These findings can improve the prediction of absolute trait responses to climate change based on the locations of genotypic origins due to local adaptation. The plasticity for growth traits, such as leaf biomass root: shoot ratio and SPR, generally increases towards higher latitudes at genotypic origins to maintain more stable physiological traits like Γ^* (Figure 6) (Molina-Montenegro and Naya 2012; Bhattarai et al. 2017; Ren et al. 2020). The RDPI in T_{opt} responding to variations in both temperature and O_2 concentration dramatically increases genotypes originating from higher latitudes, reflecting a genotype's capacity to adjust their photosynthetic machinery for optimal performance under changing climates. High plasticity indicates genotypes from high latitudes have greater ability to rapidly adapt its photosynthetic processes across a wide temperature range, commonly seen in genotypes from environments with large temperature fluctuations (Berry and Bjorkman 1980). In contrast, low plasticity suggests stable photosynthetic performance over a narrower temperature range, typical of genotypes from more thermally stable environments. This plasticity is a crucial aspect of both evolutionary adaptation and physiological acclimation, providing insights into a plant's thermal tolerance and its potential response to future climate changes. Therefore, we predict that high-latitude genotypes will be better able to cope with future climate change and frequent extreme weather events through phenotypic plasticity.

These findings highlight the complex interplay between temperature, O_2 concentration and photosynthetic processes,

13653040, 2025, 7, Downloaded from https://onlinelibrary.wiley.com/doi/10.1111/pce.15452 by East China Normal University, Wiley Online Library on [03/06/2025]. See the Terms and Conditions (https://onlinelibrary.wiley.com/terms-and-conditions) on Wiley Online Library for rules of use; OA articles are governed by the applicable Creative Commons License

underscoring the importance of considering multiple environmental factors when studying plant responses to climate change. In conclusion, we demonstrated the overall photosynthetic performance of *P. australis* is principally driven by thermal acclimation to growth temperature, comparing with the local adaptation to climate of origin. Genotypes from higher latitudes exhibited greater plasticity in temperature acclimation and photosynthetic capacity, enabling them to rapidly adjust their photosynthetic processes for optimal performance under varying thermal conditions. These insights are critical for improving the accuracy of Earth System Models, particularly in forecasting future vegetation resilience to climate change, informing conservation strategies and management practices to sustain global biodiversity and ecosystem functions.

Acknowledgements

The study was funded by the National Natural Science Foundation of China No. 42106166 (to L.R.) and No. 42141016 (to L.R. and X.L.), National Key R&D Program of China No.2023YFE0113100 (to L.R. and X.L.), China Postdoctoral Science Foundation No. 2021M700043 (to L.R.), Science and Technology Innovation Plan of Shanghai Science and Technology Commission, International scientific cooperation No. 22230713100 (to L.R., X.L. and H.B.) and Wet Horizons Horizon Europe GAP-101056848 (to H.B., B.K.S. and F.E.).

Conflicts of Interest

The authors declare no conflicts of interest.

Data Availability Statement

The data supporting the findings of this study are available in Figshare Database: 10.6084/m9. figshare.25895242.

References

Addo-Bediako, A., S. L. Chown, and K. J. Gaston. 2000. "Thermal Tolerance, Climatic Variability and Latitude." *Proceedings Biological Sciences* 267, no. 1445: 739–745.

Aguirre-Liguori, J. A., S. Ramírez-Barahona, and B. S. Gaut. 2021. "The Evolutionary Genomics of Species' Responses to Climate Change." *Nature Ecology & Evolution* 5: 1350–1360.

Angert, A. L., S. N. Sheth, and J. R. Paul. 2011. "Incorporating Population-Level Variation in Thermal Performance Into Predictions of Geographic Range Shifts." *Integrative and Comparative Biology* 51: 733–750.

Arnold, P. A., L. E. B. Kruuk, and A. B. Nicotra. 2019. "How to Analyse Plant Phenotypic Plasticity in Response to a Changing Climate." *New Phytologist* 222: 1235–1241.

Bakkenes, M., J. R. M. Alkemade, F. Ihle, R. Leemans, and J. B. Latour. 2002. "Assessing Effects of Forecasted Climate Change on the Diversity and Distribution of European Higher Plants for 2050." *Global Change Biology* 8: 390–407.

Banta, J. A., I. M. Ehrenreich, S. Gerard, et al. 2012. "Climate Envelope Modelling Reveals Intraspecific Relationships Among Flowering Phenology, Niche Breadth and Potential Range Size in *Arabidopsis thaliana*." *Ecology Letters* 15: 769–777.

Bartoń, Kamil 2020. MuMIn: Multi-Model Inference. R Package Version 1.43.17. https://CRAN.R-project.org/package=MuMIn.

Bates, D., M. Mächler, B. Bolker, and S. Walker 2015. lme4: Linear Mixed-Effects Models using 'Eigen' and S4. R Package Version 1.1-26. https://CRAN.R-project.org/package=lme4.

Battaglia, M., C. Beadle, and S. Loughhead. 1996. "Photosynthetic Temperature Responses of *Eucalyptus globulus* and *Eucalyptus nitens*." *Tree Physiology* 16: 81–89.

Bernacchi, C. J., E. L. Singsaas, C. A. R. L. O. S. Pimentel, A. R. Portis, Jr., and S. P. Long. 2001. "Improved Temperature Response Functions for Models of Rubisco-Limited Photosynthesis." *Plant, Cell & Environment* 24, no. 2: 253–259.

Berry, J., and O. Bjorkman. 1980. "Photosynthetic Response and Adaptation to Temperature in Higher Plants." *Annual Review of Plant Physiology* 31: 491–543.

Bennett, J. M., J. Sunday, P. Calosi, et al. 2021. "The Evolution of Critical Thermal Limits of Life on Earth." *Nature Communications* 12, no. 1: 1198.

Bestion, E., J. Clobert, and J. Cote. 2015. "Dispersal Response to Climate Change: Scaling Down to Intraspecific Variation." *Ecology Letters* 18: 1226–1233.

Bhattarai, G. P., L. A. Meyerson, J. Anderson, D. Cummings, W. J. Allen, and J. T. Cronin. 2017. "Biogeography of a Plant Invasion: Genetic Variation and Plasticity in Latitudinal Clines for Traits Related to Herbivory." *Ecological Monographs* 87: 57–75.

Bolnick, D. I., R. Svanbäck, J. A. Fordyce, et al. 2003. "The Ecology of Individuals: Incidence and Implications of Individual Specialization." *American Naturalist* 161: 1–28.

Busch, F. A., and R. F. Sage. 2017. "The Sensitivity of Photosynthesis to O_2 and CO_2 Concentration Identifies Strong Rubisco Control Above the Thermal Optimum." *New Phytologist* 213: 1036–1051.

von Caemmerer, S., and G. D. Farquhar. 1981. "Some Relationships Between the Biochemistry of Photosynthesis and the Gas Exchange of Leaves." *Planta* 153: 376–387.

Cen, Y. P., and R. F. Sage. 2005. "The Regulation of Rubisco Activity in Response to Variation in Temperature and Atmospheric CO_2 Partial Pressure in Sweet Potato." *Plant Physiology* 139: 979–990.

Chown, S. L., K. J. Gaston, and D. Robinson. 2004. "Macrophysiology: Large-Scale Patterns in Physiological Traits and Their Ecological Implications." *Functional Ecology* 18, no. 2: 159–167.

Climate Champions, C. 2023. The IPCC Just Published Its Summary of 5 Years of Reports–Here's What You Need to Know.

Crous, K. Y., J. Uddling, and M. G. De Kauwe. 2022. "Temperature Responses of Photosynthesis and Respiration in Evergreen Trees From Boreal to Tropical Latitudes." *New Phytologist* 234: 353–374.

Dusenge, M. E., A. G. Duarte, and D. A. Way. 2019. "Plant Carbon Metabolism and Climate Change: Elevated CO_2 and Temperature Impacts on Photosynthesis, Photorespiration and Respiration." *New Phytologist* 221: 32–49.

Duursma, R. A. 2015. "Plantecophys-An R Package for Analysing and Modelling Leaf Gas Exchange Data." *PLoS One* 10: 0143346.

Eller, F., H. Skálová, J. S. Caplan, et al. 2017. "Cosmopolitan Species as Models for Ecophysiological Responses to Global Change: The Common Reed *Phragmites australis*." *Frontiers in Plant Science* 8: 1833.

Farquhar, G. D., S. von Caemmerer, and J. A. Berry. 1980. "A Biochemical Model of Photosynthetic CO_2 Assimilation in Leaves of C3 Species." *Planta* 149: 78–90.

Fournier-Level, A., A. Korte, M. D. Cooper, M. Nordborg, J. Schmitt, and A. M. Wilczek. 2011. "A Map of Local Adaptation in *Arabidopsis thaliana*." *Science* 334: 86–89.

Fox, J., and S. Weisberg. 2019. "Car: Companion to Applied Regression." *R Package Version 3*: 0–10. https://CRAN.R-project.org/package=car.

Galmés, J., M. V. Kapralov, P. J. Andralojc, et al. 2014. "Expanding Knowledge of the Rubisco Kinetics Variability in Plant Species: Environmental and Evolutionary Trends." *Plant, Cell & Environment* 37: 1989–2001.

13653040, 2025, 7, Downloaded from https://onlinelibrary.wiley.com/doi/10.1111/pce.15452 by East China Normal University, Wiley Online Library on [03/06/2025]. See the Terms and Conditions (https://onlinelibrary.wiley.com/terms-and-conditions) on Wiley Online Library for rules of use; OA articles are governed by the applicable Creative Commons License

Gerken, A. R., O. C. Eller, D. A. Hahn, and T. J. Morgan. 2015. "Constraints, Independence, and Evolution of Thermal Plasticity: Probing Genetic Architecture of Long- and Short-Term Thermal Acclimation." *Proceedings of the National Academy of Sciences of the United States of America* 112: 4399–4404.

Gunderson, C. A., K. H. O'hara, C. M. Campion, A. V. Walker, and N. T. Edwards. 2010. "Thermal Plasticity of Photosynthesis: The Role of Acclimation in Forest Responses to a Warming Climate." *Global Change Biology* 16: 2272–2286.

Harley, P. C., and T. D. Sharkey. 1991. "An Improved Model of C3 Photosynthesis at High Co_2: Reversed O_2 Sensitivity Explained by Lack of Glycerate Reentry Into the Chloroplast." *Photosynthesis Research* 27: 169–178.

Hesketh, J. 1967. "Enhancement of Photosynthetic CO_2 Assimilation in the Absence of Oxygen, as Dependent Upon Species and Temperature." *Planta* 76: 371–374.

Husson, F., J. Josse, S. Lê, and J. Mazet. 2020. "factoMineR: Multivariate Exploratory Data Analysis and Data Mining." *R Package Version* 2: 4. https://CRAN.R-project.org/package=factoMineR.

Ikeda, D. H., T. L. Max, G. J. Allan, M. K. Lau, S. M. Shuster, and T. G. Whitham. 2017. "Genetically Informed Ecological Niche Models Improve Climate Change Predictions." *Global Change Biology* 23: 164–176.

IPCC. 2018. Global Warming of 1.5°C. An IPCC Special Report on the Impacts of Global Warming of 1.5°C Above Pre-Industrial Levels and Related Global Greenhouse Gas. Emission Pathways, in the Context of Strengthening the Global Response to the Threat of Climate Change, Sustainable Development, and Efforts to Eradicate Poverty.

Janzen, D. H. 1967. "Why Mountain Passes Are Higher in the Tropics." *American Naturalist* 101: 233–249.

Joshi, J., B. Schmid, M. C. Caldeira, et al. 2001. "Local Adaptation Enhances Performance of Common Plant Species." *Ecology Letters* 4: 536–544.

Jump, A. S., and J. Peñuelas. 2005. "Running to Stand Still: Adaptation and the Response of Plants to Rapid Climate Change." *Ecology Letters* 8: 1010–1020.

Kassambara, A., and F. Mundt 2020. factoextra: Extract and Visualize the Results of Multivariate Data Analyses. R Package Version 1.0.7. https://CRAN.R-project.org/package=factoextra.

Kattge, J., and W. Knorr. 2007. "Temperature Acclimation in a Biochemical Model of Photosynthesis: A Reanalysis of Data From 36 Species." *Plant, Cell & Environment* 30, no. 9: 1176–1190.

Kristensen, T. N., T. Ketola, and I. Kronholm. 2020. "Adaptation to Environmental Stress at Different Timescales." *Annals of the New York Academy of Sciences* 1476: 5–22.

Kriticos, D. J., B. L. Webber, A. Leriche, et al. 2012. CliMond: Global High-Resolution Historical and Future Scenario Climate Surfaces for Bioclimatic Modelling. 3, 53–64.

Kumarathunge, D. P., B. E. Medlyn, J. E. Drake, et al. 2019. "Acclimation and Adaptation Components of the Temperature Dependence of Plant Photosynthesis at the Global Scale." *New Phytologist* 222: 768–784.

Lambers, H., and R. S. Oliveira. 2019. "Photosynthesis, Respiration, and Long-Distance Transport: Photosynthesis." In *Plant Physiological Ecology*, 11–114. Springer International Publishing Cham.

Lambertini, C., B. K. Sorrell, T. Riis, B. Olesen, and H. Brix. 2012. "Exploring the Borders of European Phragmites Within a Cosmopolitan Genus." *AoB Plants* 2012: pls020.

Lancaster, L. T., and A. M. Humphreys. 2020. "Global Variation in the Thermal Tolerances of Plants." *Proceedings of the National Academy of Sciences* 117: 13580–13587.

Ma, H., L. Mo, T. W. Crowther, et al. 2021. "The Global Distribution and Environmental Drivers of Aboveground Versus Belowground Plant Biomass." *Nature Ecology & Evolution* 5: 1110–1122.

Miner, B. G., S. E. Sultan, S. G. Morgan, D. K. Padilla, and R. A. Relyea. 2005. "Ecological Consequences of Phenotypic Plasticity." *Trends in Ecology & Evolution* 20: 685–692.

Molina-Montenegro, M. A., and D. E. Naya. 2012. "Latitudinal Patterns in Phenotypic Plasticity and Fitness-Related Traits: Assessing the Climatic Variability Hypothesis (CVH) With an Invasive Plant Species." *PLoS One* 7: e47620.

Nicotra, A. B., O. K. Atkin, S. P. Bonser, et al. 2010. "Plant Phenotypic Plasticity in a Changing Climate." *Trends in Plant Science* 15: 684–692.

Niu, S., Z. Li, J. Xia, Y. Han, M. Wu, and S. Wan. 2008. "Climatic Warming Changes Plant Photosynthesis and Its Temperature Dependence in a Temperate Steppe of Northern China." *Environmental and Experimental Botany* 63, no. 1–3: 91–101.

Ogren, E. 1993. "Convexity of the Photosynthetic Light-Response Curve in Relation to Intensity and Direction of Light During Growth." *Plant Physiology* 101: 1013–1019.

Pau, S., E. M. Wolkovich, B. I. Cook, et al. 2011. "Predicting Phenology by Integrating Ecology, Evolution and Climate Science." *Global Change Biology* 17: 3633–3643.

Pinheiro, J., D. Bates, S. DebRoy, D. Sarkar, and R. Core Team. 2020. "nlme: Linear and Nonlinear Mixed Effects Models." *R Package Version* 3: 1–152. https://CRAN.R-project.org/package=nlme.

Pither, J. 2003. "Climate Tolerance and Interspecific Variation in Geographic Range Size." *Proceedings of the Royal Society of London. Series B: Biological Sciences* 270: 475–481.

R Core Team. 2021. R: A Language and Environment for Statistical Computing. R Foundation for Statistical Computing. https://www.R-project.org/.

Prioul, J. L., and P. Chartier. 1977. "Partitioning of Transfer and Carboxylation Components of Intracellular Resistance to Photosynthetic CO2 Fixation: A Critical Analysis of the Methods Used." *Annals of Botany* 41, no. 4: 789–800.

Reed, T. E., D. E. Schindler, and R. S. Waples. 2011. "Interacting Effects of Phenotypic Plasticity and Evolution on Population Persistence in a Changing Climate." *Conservation Biology* 25: 56–63.

Ren, L., X. Guo, and S. Liu, et al. 2020. "Intraspecific Variation in *Phragmites australis*: Clinal Adaption of Functional Traits and Phenotypic Plasticity Vary With Latitude of Origin." *Journal of Ecology* 108: 2531–2543.

Ren, L., X. Guo, B. K. Sorrell, F. Eller, and H. Brix. 2025. "Responses to Cold Temperature Determine Clinal Patterns of Photosynthetic Acclimation of a Cosmopolitan Grass Genus and Challenge the Concept of Quantifying Phenotypic Plasticity." *Functional Ecology* 39: 583–595.

Rivero, R. M., R. Mittler, E. Blumwald, and S. I. Zandalinas. 2022. "Developing Climate-Resilient Crops: Improving Plant Tolerance to Stress Combination." *Plant Journal* 109: 373–389.

Sage, R., T. Sharkey, and R. Pearcy. 1990. "The Effect of Leaf Nitrogen and Temperature on the CO_2 Response of Photosynthesis in the C3 Dicot *Mchenopodium album* L." *Functional Plant Biology* 17: 135–148.

Sage, R. F., and D. S. Kubien. 2007. "The Temperature Response of C3 and C4 Photosynthesis." *Plant, Cell & Environment* 30: 1086–1106.

Sage, R. F., and T. D. Sharkey. 1987. "The Effect of Temperature on the Occurrence of O_2 and CO_2 Insensitive Photosynthesis in Field Grown Plants." *Plant Physiology* 84: 658–664.

Saltonstall, K. 2002. "Cryptic Invasion by a Non-Native Genotype of the Common Reed, *Phragmites australis*, Into North America." *Proceedings of the National Academy of Sciences* 99: 2445–2449.

Santamaría, L., J. Figuerola, J. J. Pilon, et al. 2003. "Plant Performance Across Latitude: The Role of Plasticity and Local Adaptation in an Aquatic Plant." *Ecology* 84: 2454–2461.

13653040, 2025, 7, Downloaded from https://onlinelibrary.wiley.com/doi/10.1111/pce.15452 by East China Normal University, Wiley Online Library on [03/06/2025]. See the Terms and Conditions (https://onlinelibrary.wiley.com/terms-and-conditions) on Wiley Online Library for rules of use; OA articles are governed by the applicable Creative Commons License

Sasaki, M. C., and H. G. Dam. 2019. "Integrating Patterns of Thermal Tolerance and Phenotypic Plasticity With Population Genetics to Improve Understanding of Vulnerability to Warming in a Widespread Copepod." *Global Change Biology* 25: 4147–4164.

Scafaro, A. P., S. Xiang, B. M. Long, et al. 2017. "Strong Thermal Acclimation of Photosynthesis in Tropical and Temperate Wet-Forest Tree Species: The Importance of Altered Rubisco Content." *Global Change Biology* 23, no. 7: 2783–2800.

Sharkey, T. D. 1988. "Estimating the Rate of Photorespiration in Leaves." *Physiologia Plantarum* 73: 147–152.

Smith, N. G., and T. F. Keenan. 2020. "Mechanisms Underlying Leaf Photosynthetic Acclimation to Warming and Elevated CO_2 as Inferred From Least-Cost Optimality Theory." *Global Change Biology* 26: 5202–5216.

Stevens, G. C. 1989. "The Latitudinal Gradient in Geographical Range: How So Many Species Coexist in the Tropics." *American Naturalist* 133: 240–256.

Sunday, J., J. M. Bennett, P. Calosi, et al. 2019. "Thermal Tolerance Patterns Across Latitude and Elevation." *Philosophical Transactions of the Royal Society B* 374, no. 1778: 20190036.

Thuiller, W., S. Lavorel, and M. B. Araújo. 2005. "Niche Properties and Geographical Extent as Predictors of Species Sensitivity to Climate Change." *Global Ecology and Biogeography* 14: 347–357.

Turner, M. G., W. J. Calder, G. S. Cumming, et al. 2020. "Climate Change, Ecosystems and Abrupt Change: Science Priorities." *Philosophical Transactions of the Royal Society, B: Biological Sciences* 375: 20190105.

Valladares, F., E. Gianoli, and J. M. Gómez. 2007. "Ecological Limits to Plant Phenotypic Plasticity." *New Phytologist* 176: 749–763.

Valladares, F., S. Matesanz, F. Guilhaumon, et al. 2014. "The Effects of Phenotypic Plasticity and Local Adaptation on Forecasts of Species Range Shifts Under Climate Change." *Ecology Letters* 17: 1351–1364.

Walker, B., L. S. Ariza, S. Kaines, M. R. Badger, and A. B. Cousins. 2013. "Temperature Response of In Vivo Rubisco Kinetics and Mesophyll Conductance in *Arabidopsis thaliana*: Comparisons to *Nicotiana tabacum*." *Plant, Cell & Environment* 36: 2108–2119.

Wang, H., O. K. Atkin, T. F. Keenan, et al. 2020. "Acclimation of Leaf Respiration Consistent With Optimal Photosynthetic Capacity." *Global Change Biology* 26, no. 4: 2573–2583.

Wessely, J., A. Gattringer, F. Guillaume, et al. 2022. "Climate Warming May Increase the Frequency of Cold-Adapted Haplotypes in Alpine Plants." *Nature Climate Change* 12: 77–82.

Wingler, A., P. J. Lea, W. P. Quick, and R. C. Leegood. 2000. "Photorespiration: Metabolic Pathways and Their Role in Stress Protection." *Philosophical Transactions of the Royal Society of London. Series B: Biological Sciences* 355, no. 1402: 1517–1529.

Yamori, W., K. Hikosaka, and D. A. Way. 2014. "Temperature Response of Photosynthesis in C3, C4, and CAM Plants: Temperature Acclimation and Temperature Adaptation." *Photosynthesis Research* 119: 101–117.

Yamori, W., K. Noguchi, K. Hikosaka, and I. Terashima. 2010. "Phenotypic Plasticity in Photosynthetic Temperature Acclimation Among Crop Species With Different Cold Tolerances." *Plant Physiology* 152, no. 1: 388–399.

Zhu, L., K. J. Bloomfield, C. H. Hocart, et al. 2018. "Plasticity of Photosynthetic Heat Tolerance in Plants Adapted to Thermally Contrasting Biomes." *Plant, Cell & Environment* 41, no. 6: 1251–1262.

Zuur, A., E. N. Ieno, N. Walker, A. A. Saveliev, and G. M. Smith. 2009. *Mixed Effects Models and Extensions in Ecology With R*. Springer.

Supporting Information

Additional supporting information can be found online in the Supporting Information section.

13653040, 2025, 7, Downloaded from https://onlinelibrary.wiley.com/doi/10.1111/pce.15452 by East China Normal University, Wiley Online Library on [03/06/2025]. See the Terms and Conditions (https://onlinelibrary.wiley.com/terms-and-conditions) on Wiley Online Library for rules of use; OA articles are governed by the applicable Creative Commons License